Asian Journal of Chemistry; Vol. 34, No. 10 (2022), 2688-2696

ASIAN JOURNAL OF CHEMISTRY

https://doi.org/10.14233/ajchem.2022.23911

4*f*-4*f* Transition Spectra of the Interaction of Pr(III) with L-Valine in Solution: Kinetics and Thermodynamic Studies

JULIANA SANCHU, MHASIRIEKHO ZIEKHRÜ, ZEVIVONÜ THAKRO and M.I. DEVI*

Department of Chemistry, Nagaland University, Lumami-798627, India

*Corresponding author: E-mail: cam_indira@yahoo.co.in

Received: 14 May 2022; *Accepted*: 28 July 2022; *Published online*: 19 September 2022; AJC-20975

The 4*f*-4*f* transition spectra for the interaction of L-valine with praseodymium(III) in aqueous organic solvents (50% v/v) of CH_3CN, DMF, CH_3OH and $C_4H_8O_2$ is investigated. The variation in the theoretically computed values of the absorption spectral parameters *viz*. energy interaction parameters-spin-orbit interaction (ξ_{4f}), Slater-Condon (F_k), nephelauxetic ratio (β), Racah energy (E_k), bonding parameter ($b^{1/2}$) and percentage covalency (δ) explained the nature of complexation. The values of evaluated intensity parameters *viz*. oscillator strengths (P) and Judd-Ofelt parameters (Ω_t) (t = 2, 4, 6) were analyzed to see the possibility of outer and inner sphere coordination of Pr(III) with L-valine. Further, reaction pathways for Pr(III) with L-valine and consequently its thermodynamic parameters have been evaluated through 4*f*-4*f* transition spectra in the DMF solvent.

Keywords: Oscillator strength, Nephelauxetic effect, Pr(III), Judd-Ofelt, Thermodynamic parameters.

INTRODUCTION

Lanthanide(III) with ligands like amino acids or peptides and their bonding character are being studied within the field of biological chemistry because of their potential utility as structural probes [1-3]. Lanthanides are important in a variety of areas, including organic and bioorganic chemistry, optical sensing technologies (such as luminescence sensors) and medicine (diagnostic and therapy), with medical applications developing rapidly in recent years. The fact that lanthanides, with their unique 4*f*-electron configuration, have coordination numbers ranging from 6 to 12 justifies their vast range of uses. Rare earth ions have antibacterial, anticancer and antiviral properties when combined with organic ligands and they play a significant role in many essential biological processes [4-6]. Because of their enthralling and important characteristics, such as their capability to attach to nitrogen, oxygen and skeletal probes in biological systems, lanthanide complexes have received a great deal of research interest. A comprehensive analysis of the interactions of several lanthanides with a wide range of proteins, amino acids and polypeptides has been reported [7]. Because of the lanthanide's paramagnetic properties, which make it spectroscopically active, the lanthanide(III) complex can provide important details regarding how it interacts with amino acids [8-10]. As lanthanides are utilized more often as probes to examine the structural function of biomolecular processes, their coordinating chemistry in solution is fast emerging [11-13].

Lanthanides favour the donor atoms O > N > S and F > Cl in the complexation. This shows a high preference for 'O' donor atoms by lanthanides. As long as the side chains (-R group) of amino acids are present, their functional groups ($-NH_2$ & -COOH) can be employed to change the shape and size of positive materials [14]. Peptides and amino acids are frequent macromolecules that function as efficient metal binding sites in physiological conditions. Simple amino acid building blocks make up peptides, which have a wide spectrum of biological significance. Due to its therapeutic qualities, peptide research is one of the most popular areas of study [15]. The relationship between Ln(III) ions and amino acids is well known; the lanthanide ion is attached to the oxygen atom of carboxylato group and the nitrogen atom of amino group [16]. When amino acids are solid, they are in a state of neutrality. They exist as zwitter ions in an aqueous solution if their isoelectric point is maintained [17,18], as seen in Fig. 1. Thus, using a probe (4*f*-4*f* spectra) of praseodymium(III) to understand the interaction

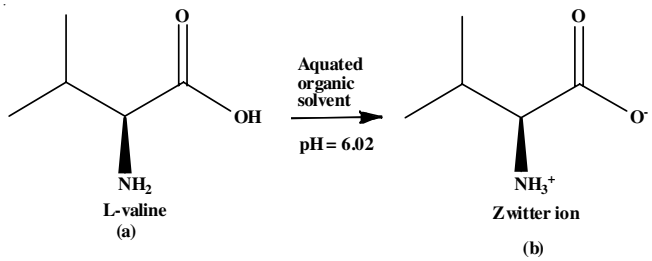

Fig. 1. Structure of L-valine in its free state and zwitterion form

of the ligand with the metal ion would be a fascinating scope to investigate in detail.

By employing the 4*f*-4*f* spectra of praseodymium(III) as a probe, the current study explores the complexation between the praseodymium(III) ion and L-valine in the binary mixtures of water and organic solvents (CH_3CN, DMF, $C_4H_8O_2$ and CH_3OH). The fluctuations in the theoretically determined values of the energy parameters *viz.*, Slater-Condon (F_k), spin-orbit interaction (ξ_{4f}), Racah energy (E_k), nephelauxetic ratio (β), bonding parameter ($b^{1/2}$) and percentage covalency (δ) were used to investigate the complexity of the complexation. The oscillator strengths (P) and Judd-Ofelt parameters Ω_t (t = 2, 4, 6) used to measure intensity were analyzed. The variations in P and Ω_t (t = 2, 4, 6) values show a specific correlation between relative intensities, ion behaviour toward solvents, ligand structures and complexation nature. By calculating the parameters such as rate constant (k), ΔH°, ΔS°, ΔG° and frequency factor (A), it is possible to analyze the thermodynamic behaviour as well as the pathways of the reaction.

EXPERIMENTAL

Pr(III) chloride hydrate [$PrCl_3 \cdot xH_2O$] of 99.9% purity was purchased from Alfa-Aesar and the ligand *i.e.* L-valine was purchased from HIMEDIA. The solvents used were DMF, acetonitrile, methanol, 1,4-dioxane and of AR grade. The concentration of solutions for recording spectra was maintained at 10^{-2} M.

For kinetic investigations, a 10^{-2} M concentration of Pr(III) and L-valine combination was prepared in DMF solvent. At various temperatures, all spectra were recorded from 400-700 nm using a temperature-controlled Perkin-Elmer Lambda-35 UV-visible spectrophotometer with related kinetic assembly. Using a water-circulating HAAKE DC 10 Thermostat, all of the observations are kept at the same temperature. The energy bands are determined using Judd [19] and Ofelt [20] theoretical treatment.

Theoretical

Energy interaction and intensity parameters: For Pr(III) complexes, the values of interelectronic parameters, *i.e.* F_2, F_4, F_6 and ξ_{4f} were determined by using the technique developed by Mishra *et al.* [21].

$$E_{obs} = E_{oj} + \frac{\delta E_j}{\delta F_2}\Delta F_2 + \frac{\delta E_j}{\delta \xi_{4f}}\Delta \xi_{4f} \quad (1)$$

The partial regression approach is then used to obtain estimated F_2 and ξ_{4f} values. The following relationship yields approximate F_4 and F_6 values:

$$\frac{F_4}{F_2} = 0.13805 \text{ and } \frac{F_6}{F_2} = 0.151 \quad (2)$$

Nephelauxetic ratio (β) measures the change in F_k w.r.t. free ion, which is defined as:

$$\beta_1 = \frac{F_k^c}{F_k^f}; \beta_2 = \frac{\xi_{4f}^c}{\xi_{4f}^f} \text{ and } \beta = \left(\frac{\beta_1 + \beta_2}{2}\right) \quad (3)$$

where F_c^k and F_k^f refer to parameters in free ion and complex, respectively.

Another bonding measure ($b^{1/2}$) related to the nephelauxetic effect (β) can be used to determine the degree of mixing between the 4*f*-orbital and the ligand orbital as:

$$b^{1/2} = \left(\frac{1-\beta}{2}\right)^{1/2} \quad (4)$$

Sinha [22] introduced another parameter known as the percentage covalency parameter (δ%), which is defined as:

$$\delta\ (\%) = \left(\frac{1-\beta}{\beta}\right) \times 100 \quad (5)$$

The area under the absorption curve and the oscillator strength (P) are directly related and is represented as:

$$P = 4.6 \times 10^{-9}\left(\frac{9\eta}{(\eta^2+\eta)^2}\right)\int \varepsilon_{max}\bar{\nu}d\bar{\nu} \quad (6)$$

where ε_{max} = molar extinction coefficient, $\bar{\nu}$ = transition energy in wave number and η = refractive index of the medium.

The experimental value of oscillator strengths (P_{obs}) of absorption band determined *via* Gaussian curve analysis is:

$$P_{obs} = 4.6 \times 10^{-9} \times \varepsilon_{max} \times \bar{\nu}_{1/2} \quad (7)$$

The transition energies' observed oscillator strength (P_{obs}) was expressed in terms of t_2, t_4 and t_6 parameters provided by Judd [19] and Ofelt [20], which are supplied:

$$\frac{P_{obs}}{\nu} = [(U^2)]^2 t_2 + [(U^4)]^2 t_4 + [(U^6)]^2 t_6 \quad (8)$$

where U^λ is the matrix element given by Carnall *et al.* [23] and v is the transition energy.

Evaluation of thermodynamic parameters: Using the Arrhenius rate equation [24] by graphing log k *versus* 1/T, it is used to calculate the activation energy for the complexation of praseodymium(III) and L-valine.

$$\log k - \log A - \frac{E_a}{2.303R} \times \frac{1}{T} \quad (9)$$

From the slope, the activation energy E_a is given by:

$$E_a = -2.303 \times R \times \text{Slope} \quad (10)$$

where R = universal gas constant.

The thermodynamic features for praseodymium(III): L-valine complex was evaluated using Van't Hoff [25] equation of log k *vs.* $1/T \times 10^3$

$$\log k = -\frac{\Delta H^\circ}{R}\left(\frac{1}{T}\right) + \frac{\Delta S^\circ}{R}$$

or

$$\log k = -\frac{\Delta G^\circ}{RT} \quad (11)$$

RESULTS AND DISCUSSION

Deep within the metal's core cell, non-hypersensitive transitions are assumed to be insensitive to the coordination environment [25]. The hypersensitive transitions, on the other hand, are extremely receptive to changes in their coordination sphere and conform to the selection criteria, when Ln(III) complexes with ligand [26]. Studies have shown that some Pr(III) transition intensities ($^3H_4 \rightarrow {}^3P_2$, $^3P_1$, $^3P_0$ and $^1D_2$) do not follow the selection criteria but are extraordinarily sensitive to even the smallest variations in their coordinating surroundings. Because of how their coordinated environment affects their sensitivity, these pseudoquadrupole transitions are also known as ligand mediated pseudo hypersensitive transitions [23,27,28]. To study the structural conformations and interactions of Pr(III) with ligand, this pseudo-hypersensitive transition has been widely exploited in solution absorption studies [25].

Table-1 shows that when L-valine was added to Pr(III), the Slater-Condon (F_k) (k = 2,4,6) and spin-orbit interaction (ξ_{4f}) decreases, indicating a decrease in both spin-orbit interaction and coulombic parameters, resulting in an expansion of the central metal ion orbital and a decrease in the metal-ligand bond distance, allowing complexation. The nephelauxetic effect (β) in all systems ranges between 0.944-0.947, which is less than unity, indicating the validity of the computed data. The values of bonding parameters ($b^{1/2}$) are positive, with increasing values of Sinha's parameter (δ) indicating the possibility of covalent bonding. It is based on the earlier stated notion of *f-f* transition [29]. Table-2 shows the calculated and observed values of energy for the different bands and the value of root mean square deviation (RMS) indicates how close to the accuracy of the evaluated data.

The intensity parameters 'P' and 'Ω_t' (t = 2, 4, 6) for the transitions ($^3H_4 \rightarrow {}^3P_2$, $^3P_1$, $^3P_0$ and $^1D_2$) of free Pr(III) and Pr(III): L-valine complex in various aquated organic solvents were evaluated. The remarkable increases in the 'P' values as shown in Table-3 suggest the possibility of Pr(III) and L-valine interaction. When complexation occurs between Pr(III) and L-valine in solution, the values of 'Ω_t' parameters increases significantly, the possibility of binding of L-valine to Pr(III). t_4 and t_6 are significantly affected and their values are positive, allowing them to be used in the Judd-Ofelt hypothesis. Large fluctuations in the magnitudes of the t_4 and t_6 parameters suggest the possible modifications of the coordination spheres that surround them and also the possible influence how Pr(III) interacts with its ligands. Both t_4 and t_6 parameters are connected

TABLE-1
COMPARISON OF ENERGY INTERACTION VALUES: SLATER-CONDON (F_k), LANDE (ξ_{4f}), RACAH ENERGY (E^K), NEPHELAUXETIC RATIO (β), BONDING ($b^{1/2}$) AND COVALENCY (δ) FACTORS OF Pr(III) AND Pr(III): L-VALINE COMPLEX IN DIFFERENT AQUEOUS SOLVENTS

Systems	F_2	F_4	F_6	ξ_{4f}	E^1	E^2	E^3	β	$b^{1/2}$	δ
Acetonitrile										
Pr(III)	308.471	43.721	5.757	723.62	3515.12	24.782	588.22	0.946	0.1626	5.589
Pr(III) + valine	308.303	43.698	5.678	723.60	3514.99	24.768	587.89	0.947	0.1627	5.593
Dimethylformamide										
Pr(III)	308.035	43.655	5.669	721.27	3509.62	24.748	587.38	0.945	0.165	5.754
Pr(III) + valine	308.029	43.650	5.665	720.21	3509.58	24.746	587.35	0.947	0.165	5.778
1,4-Dioxane										
Pr(III)	308.275	43.724	5.677	723.29	3512.75	24.792	588.28	0.946	0.163	5.607
Pr(III) + valine	308.270	43.722	5.674	723.22	3512.69	24.786	588.22	0.947	0.163	5.588
Methanol										
Pr(III)	308.305	43.698	5.678	722.52	3512.85	24.768	587.92	0.944	0.162	5.577
Pr(III) + valine	308.301	43.697	5.675	722.49	3511.81	24.767	587.88	0.945	0.163	5.590

TABLE-2
COMPARISON OF ENERGIES (cm^{-1}) VALUES AS WELL AS RMS VALUES FOR Pr(III) AND Pr(III): L-VALINE IN DIFFERENT AQUEOUS SOLVENTS

Systems	$^3H_4 \rightarrow {}^3P_2$		$^3H_4 \rightarrow {}^3P_1$		$^3H_4 \rightarrow {}^3P_0$		$^3H_4 \rightarrow {}^1D_2$		RMS
	E_{obs}	E_{cal}	E_{obs}	E_{cal}	E_{obs}	E_{cal}	E_{obs}	E_{cal}	
Acetonitrile									
Pr(III)	22525.06	22469.51	21351.10	21258.39	20741.72	20694.87	16975.33	17146.05	103.56
Pr(III) + valine	22524.55	22470.19	21350.36	21257.21	20740.43	20693.66	16974.76	17145.28	103.44
Dimethylformamide									
Pr(III)	22493.65	22441.63	21293.45	21231.80	20742.15	20674.09	16920.87	17122.77	103.84
Pr(III) + valine	22493.64	22441.69	21293.36	21222.04	20742.11	20666.31	16920.47	17122.07	117.21
1,4-Dioxane									
Pr(III)	22525.06	22470.04	21351.10	21258.39	20741.72	20694.04	16975.33	17146.15	103.56
Pr(III) + valine	22524.76	22470.30	21350.64	21258.42	20741.29	20694.29	16975.25	17146.51	103.60
Methanol									
Pr(III)	22525.16	22470.32	21351.10	21258.39	20741.72	20694.07	16975.33	17146.05	103.56
Pr(III) + valine	22525.06	22470.47	21351.05	21258.45	20740.59	20694.35	16974.76	17145.54	103.68

TABLE-3
COMPARISON OF OSCILLATOR STRENGTHS AND JUDD-OFELT PARAMETERS FOR Pr(III) AND Pr(III): L-VALINE COMPLEX IN DIFFERENT AQUEOUS SOLVENTS

Systems	$^3H_4 \rightarrow {}^3P_2$		$^3H_4 \rightarrow {}^3P_1$		$^3H_4 \rightarrow {}^3P_0$		$^3H_4 \rightarrow {}^1D_2$		t_2	t_4	t_6
	P_{obs}	P_{cal}	P_{obs}	P_{cal}	P_{obs}	P_{cal}	P_{obs}	P_{cal}			
Acetonitrile											
Pr(III)	18.671	18.671	5.797	4.263	2.685	4.193	3.898	3.898	-524.4	11.697	58.123
Pr(III) + valine	19.29	19.29	5.865	4.405	2.897	4.333	3.98	3.98	-595.4	12.086	60.044
Dimethylformamide											
Pr(III)	17.386	17.386	5.559	4.371	3.131	4.299	3.281	3.281	-411.8	11.992	53.831
Pr(III) + valine	20.879	20.879	5.571	4.595	3.216	4.520	3.435	3.435	-492.1	12.608	65.049
1,4-Dioxane											
Pr(III)	16.855	16.855	5.506	3.697	2.871	4.343	3.025	3.025	-356.4	12.116	52.055
Pr(III) + valine	18.022	18.022	5.861	4.639	3.674	4.574	3.883	3.883	-378.3	12.759	58.872
Methanol											
Pr(III)	16.613	16.613	5.551	4.405	1.859	3.639	2.238	2.238	-368.6	10.149	51.796
Pr(III) + valine	18.437	18.437	5.898	4.134	2.367	4.066	2.418	2.418	-400.2	11.341	55.741

to changes in the symmetry characteristics of complex species. Although the transitions $^3H_4 \rightarrow {}^3F_3$ and t_2 are associated with the hypersensitive transition, t_2 is disregarded because the transition $^3H_4 \rightarrow {}^3F_3$ has readings that are negative and outside of the ultraviolet-visible zone [30]. While modest fluctuations of P and Ω_t parameters show the outer-sphere complexation, whereas large variations in the readings of P and Ω_t parameters indicate inner-sphere complexation. The significant changes in the calculated values of P and give strong support for the involvement of L-valine in the inner-sphere coordination of Pr(III).

The comparative absorption spectra of Pr(III) and Pr(III): L-valine complex in aqueous DMF solvent are shown in Fig. 2. All of the energy bands experience a red shift when a ligand like L-valine was added, however, the changes in the intensity data were brought by the strengthening of the 4*f*-4*f* transition bands. Band intensification is thought to be diligent from increased interaction between ligand orbitals and 4*f*-metal orbitals. A reduction in the coordination number and the metal-ligand bond length may be connected to the intensification of bands, notably the $^3H_4 \rightarrow {}^3P_2$ transition. As seen in Fig. 3, the development of Pr(III):L-valine complex reveals the sensitivities of solvent shown by the varied intensities of the bands of the four transitions and the order of the sensitivity of the solvent is DMF > CH_3CN > dioxane > CH_3OH. DMF often binds through oxygen rather than nitrogen when it coordinates to hard acids, such as lanthanide ions, whereas CH_3CN binds through nitrogen. The increased intensification in the DMF medium also reveals that oxygen and nitrogen can form stronger bonds than nitrogen, that is why DMF could show the maximum intensification and hence is the best solvent. Methanol is a poor donor.

The coordination numbers and geometries are dictated largely by ligand properties such as ion generation, donor atoms, sizes and solvation effects. Lanthanide aqueous solution has a coordination number of 9 and 8, which may be increased to 12 with the addition of a ligand. Praseodymium(III) ions produce weak complexes when goes complexation with monodentate ligands, but stronger complexes when complexed with chelated ligands due to the chelate effect [31]. When an amino

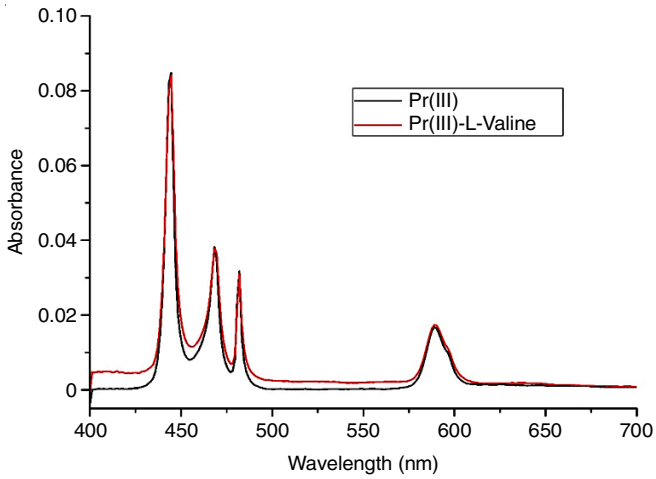

Fig. 2. Absorption spectra of Pr(III) and Pr(III):L-valine complex in aqueous DMF solvent

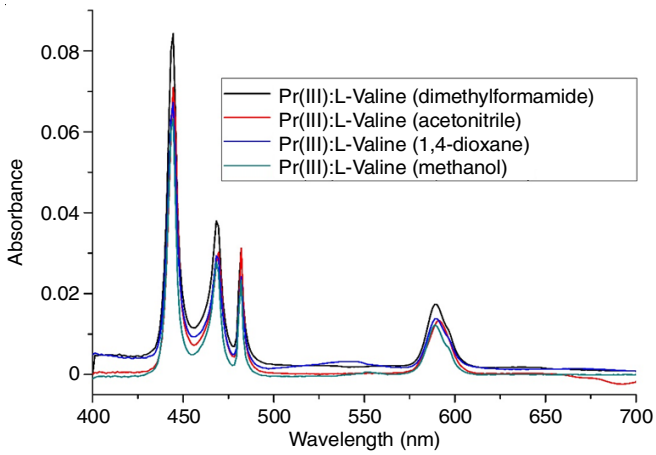

Fig. 3. Absorption spectra of Pr(III) and Pr(III): L-valine complex in various aqueous organic solvents

acid's isoelectric point is maintained, it exists in solution as a zwitter ion. Praseodymium(III) is an ionic salt and acts as a hard acceptor, whereas amino acids are hard donors. At low pH, complexation occurs between Pr(III) and the oxygen atom of the amino acid, but at high pH, the metal ion bonds to the oxygen and nitrogen atoms of the amino acid, respectively.

Praseodymium(III) ions form stable complexes with oxygen and nitrogen donor ligands, resulting in nona-coordinating complex. Fig. 4 depicts a reaction pathway for the nona-coordinated Pr(III):L-valine complex in an aquated organic solvent.

To explore the kinetics of the complexation of Pr(III) with L-valine, the absorption spectra for the complexation of Pr(III) with L-valine were recorded at various temperatures (298, 303, 308, 313 and 318 K) (Fig. 5) and time intervals in aquated DMF solvent. Based on changes in the observed and calculated values of oscillator strength and Judd Ofelt parameters at various temperatures for Pr(III):L-valine complex as shown in Tables 4-8. It is observed that the pseudo-hypersensitive transition $^3H_4 \rightarrow {}^3P_2$ is the most sensitive transition in comparison to the other $^3H_4 \rightarrow {}^3P_1$, $^3P_0$ and $^1D_2$ transitions. The plot of P_{obs} *vs.* time for the transition $^3H_4 \rightarrow {}^3P_2$ at various temperatures is shown in Fig. 6. The rate constants were calculated using the values of slope derived from the graph, as given in Table-9. Following the Arrhenius theoretical prediction, complexation rates grow with a rise in temperature as shown in Tables 4-8. Additionally, the Pre-exponential factor (A) values increasing with temperature suggests an increase in molecules colliding. The extremely low activation energy (E_a) value suggests that the reaction is a fast one. Fig. 7 also shows the graph of log k *versus* $1/T \times 10^3$, the values of ΔH°, ΔG° and ΔS° as given in Table-10 were determined from the graph.

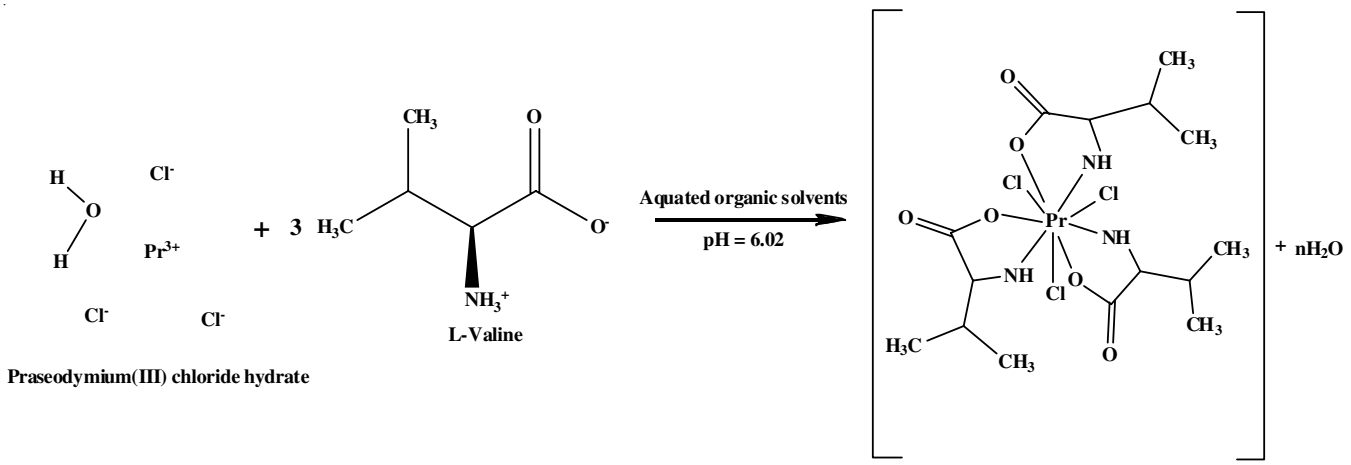

Fig. 4. Reaction pathway for nona-coordinated Pr(III): L-valine complex in an aquated organic solvent

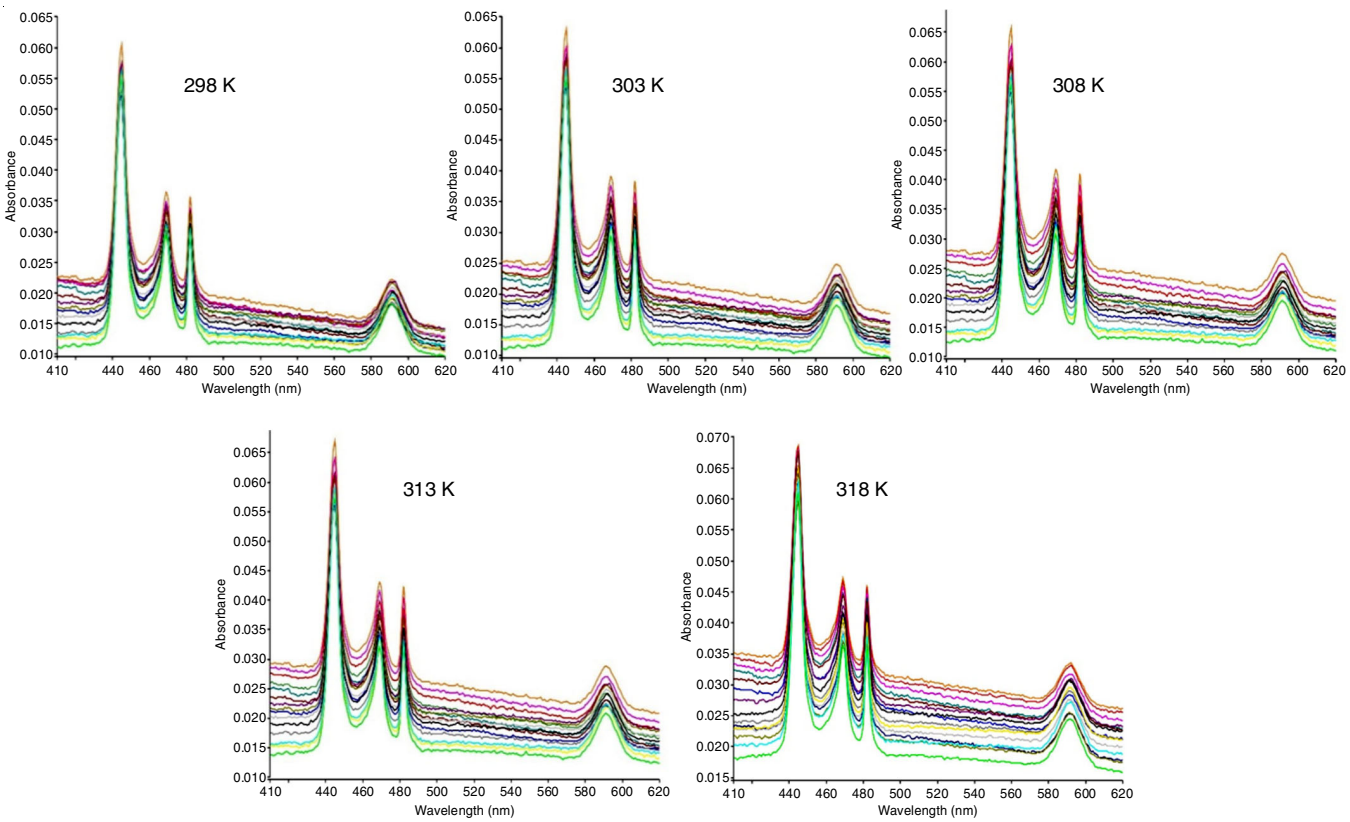

Fig. 5. Absorption spectra for the interaction of Pr(III): L-valine at various temperatures 298, 303, 308, 313 and 318 K in DMF solvent

TABLE-4
COMPUTED OSCILLATOR STRENGTHS AND JUDD-OFELT INTENSITY PARAMETER FOR Pr(III): L-VALINE COMPLEX AT 298 K IN VARIOUS TIME (h) INTERVALS

Time (h)	$^3H_4 \rightarrow {}^3P_2$		$^3H_4 \rightarrow {}^3P_1$		$^3H_4 \rightarrow {}^3P_0$		$^3H_4 \rightarrow {}^1D_2$		t_2	t_4	t_6
	P_{obs}	P_{cal}	P_{obs}	P_{cal}	P_{obs}	P_{cal}	P_{obs}	P_{cal}			
0	6.636	6.636	2.745	1.765	0.634	1.656	1.122	1.122	-180.23	4.731	20.412
2	6.678	6.678	2.915	1.913	0.755	1.787	1.357	1.357	-179.55	4.965	20.545
4	6.734	6.734	3.164	2.072	0.872	1.986	1.406	1.406	-179.87	5.342	20.672
6	6.855	6.855	3.243	2.098	0.897	2.023	1.628	1.628	-79.36	5.578	20.819
8	6.918	6.918	3.356	2.106	0.909	2.091	1.849	1.849	-39.78	5.731	21.223
10	7.116	7.116	3.361	2.142	0.949	2.126	1.884	1.884	-43.99	5.827	21.674
12	7.207	7.207	3.378	2.192	0.995	2.145	1.906	1.906	-45.78	5.965	22.123
14	7.296	7.296	3.391	2.204	1.003	2.159	1.975	1.975	-41.67	6.055	22.356
16	7.367	7.367	3.433	2.219	1.016	2.191	2.104	2.104	-134.36	6.097	22.543
18	7.475	7.475	3.482	2.271	1.042	2.213	2.338	2.338	39.05	6.173	22.812
20	7.654	7.654	3.567	2.338	1.066	2.276	2.434	2.434	48.56	6.359	23.256
22	7.734	7.734	3.712	2.456	1.096	2.341	2.543	2.543	68.02	6.534	23.786
24	8.012	8.012	3.821	2.465	1.118	2.431	2.589	2.589	49.45	6.717	24.423
26	8.094	8.094	3.872	2.572	1.135	2.487	2.641	2.641	68.78	6.856	24.876
28	8.211	8.211	3.976	2.624	1.145	2.532	2.731	2.731	87.76	6.967	25.512
30	8.376	8.376	4.199	2.687	1.231	2.631	2.897	2.97	93.67	7.234	25.854
32	8.521	8.521	4.295	2.791	1.362	2.708	3.013	3.01	102.45	7.441	26.398
34	8.889	8.889	4.387	2.867	1.456	2.829	3.201	3.20	100.67	7.653	26.875

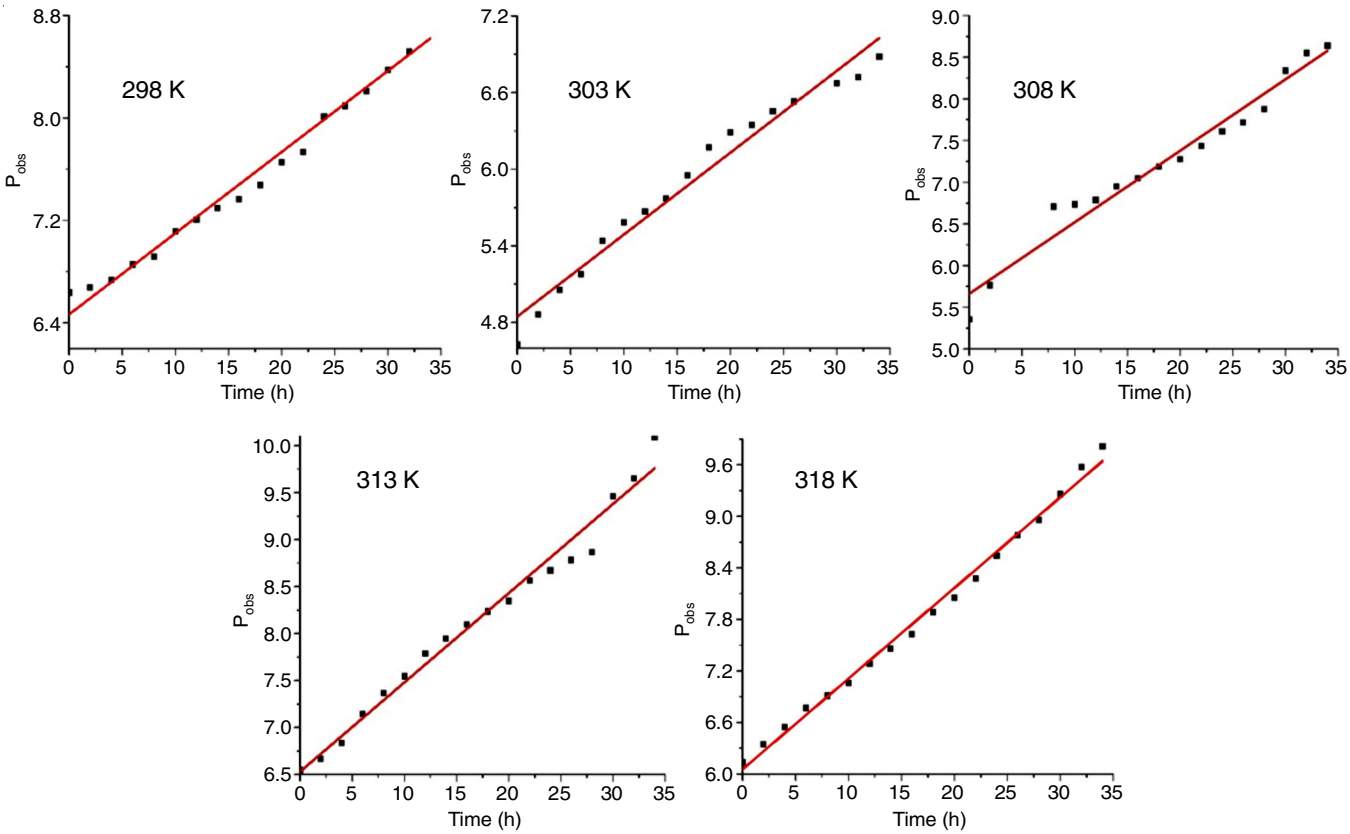

Fig. 6. Plot of oscillator strength *vs.* time (h) for $^3H_4 \rightarrow {}^3P_2$ transition for Pr(III): L-valine complex in DMF solvent at different temperatures 298, 303, 308, 313 and 318 K

The positive values of ΔHº demonstrated that the reaction is an endothermic reaction, whereas the negative value of ΔGº represents the spontaneity of the reaction process. According to the positive values of ΔSº, the complexation process is entropy-driven and the complex is well-formed. Additionally, it was found that the Pr(III):L-valine complex's activation energies (E_a) was 0.05119 kJ. These kinetic studies, based on an investigation through absorption spectrum are used as an alternate method to explore the reaction kinetics theoretically and to forecast potential thermodynamic behaviour related to the complexation of Pr(III):L-valine.

TABLE-5
COMPUTED OSCILLATOR STRENGTHS AND JUDD-OFELT INTENSITY PARAMETER FOR Pr(III): L-VALINE COMPLEX AT 303 K IN VARIOUS TIME (h) INTERVALS

Time (h)	$^3H_4 \rightarrow {}^3P_2$		$^3H_4 \rightarrow {}^3P_1$		$^3H_4 \rightarrow {}^3P_0$		$^3H_4 \rightarrow {}^1D_2$		t_2	t_4	t_6
	P_{obs}	P_{cal}	P_{obs}	P_{cal}	P_{obs}	P_{cal}	P_{obs}	P_{cal}			
0	4.629	4.629	2.519	1.857	1.153	1.834	1.717	1.717	78.187	5.145	13.841
2	4.864	4.864	2.591	1.919	1.227	1.896	1.794	1.794	78.385	5.268	14.574
4	5.055	5.055	2.623	1.959	1.259	1.912	1.822	1.822	70.866	5.373	15.162
6	5.178	5.178	2.644	1.967	1.278	1.986	1.915	1.915	89.827	5.436	15.387
8	5.439	5.439	2.765	2.065	1.341	2.025	1.997	1.997	90.855	5.663	16.319
10	5.585	5.585	2.918	2.138	1.366	2.116	2.356	2.356	170.46	5.872	16.655
12	5.667	5.667	2.935	2.163	1.389	2.122	2.523	2.523	201.66	5.965	16.786
14	5.772	5.772	2.958	2.193	1.412	2.166	2.576	2.576	207.45	6.059	17.512
16	5.954	5.954	2.987	2.214	1.462	2.191	2.646	2.646	209.76	6.182	18.154
18	6.172	6.172	3.056	2.294	1.523	2.242	2.782	2.782	210.87	6.271	18.587
20	6.287	6.287	3.178	2.379	1.577	2.383	3.009	3.009	269.76	6.545	18.842
22	6.345	6.345	3.352	2.482	1.634	2.462	3.045	3.045	272.66	6.739	19.063
24	6.456	6.456	3.467	2.639	1.701	2.571	3.095	3.095	267.52	7.179	19.267
26	6.531	6.531	3.681	2.744	1.795	2.683	3.187	3.187	283.12	7.461	19.396
28	6.569	6.569	3.782	2.798	1.804	2.725	3.298	3.298	309.69	7.673	19.544
30	6.672	6.672	3.863	2.859	1.813	2.784	3.495	3.495	346.31	7.791	19.683
32	6.723	6.723	3.887	2.946	1.967	2.855	3.565	3.565	360.88	8.158	19.881
34	6.881	6.881	4.123	3.106	2.245	2.983	3.884	3.884	410.59	8.374	20.218

TABLE-6
COMPUTED OSCILLATOR STRENGTHS AND JUDD-OFELT INTENSITY PARAMETER FOR Pr(III): L-VALINE COMPLEX AT 308 K IN VARIOUS TIME (h) INTERVALS

Time (h)	$^3H_4 \rightarrow {}^3P_2$		$^3H_4 \rightarrow {}^3P_1$		$^3H_4 \rightarrow {}^3P_0$		$^3H_4 \rightarrow {}^1D_2$		t_2	t_4	t_6
	P_{obs}	P_{cal}	P_{obs}	P_{cal}	P_{obs}	P_{cal}	P_{obs}	P_{cal}			
0	5.355	5.355	1.183	1.189	1.003	1.056	2.467	2.467	219.55	2.475	16.854
2	5.767	5.767	1.372	1.156	1.072	1.155	2.574	2.581	209.52	3.431	18.571
4	6.605	6.605	3.168	2.187	1.155	2.147	1.116	1.116	-185.21	5.459	20.712
6	6.679	6.679	3.247	2.233	1.204	2.246	1.187	1.187	-173.65	6.234	20.129
8	6.706	6.706	2.756	1.997	1.235	1.969	1.248	1.248	-166.36	5.493	20.621
10	6.735	6.735	2.764	2.008	1.251	1.993	1.317	1.329	-148.51	5.542	20.682
12	6.787	6.787	2.767	2.041	1.285	2.007	1.383	1.381	-138.23	5.651	20.843
14	6.951	6.951	2.789	2.113	1.336	2.182	1.406	1.406	-141.59	5.771	21.273
16	7.046	7.046	3.143	2.236	1.407	2.248	1.875	1.875	-136.26	6.243	21.345
18	7.187	7.187	3.245	2.366	1.449	2.308	1.961	1.961	-37.83	6.461	21.783
20	7.276	7.276	3.316	2.451	1.494	2.427	2.083	2.083	-16.67	6.726	22.082
22	7.437	7.437	3.455	2.570	1.584	2.490	2.121	2.121	-22.83	6.969	22.813
24	7.609	7.609	3.527	2.553	1.636	2.576	2.195	2.195	-9.39	7.183	23.126
26	7.716	7.716	3.617	2.642	1.656	2.631	2.491	2.491	43.91	7.327	23.648
28	7.878	7.878	3.727	2.732	1.689	2.685	2.578	2.578	57.19	7.464	23.838
30	8.339	8.339	4.445	3.134	1.715	3.123	2.623	2.623	65.57	8.531	25.118
32	8.549	8.549	5.423	3.284	1.786	3.405	2.787	2.787	66.26	9.562	25.339
34	8.637	8.637	5.905	3.845	1.855	3.806	3.099	3.099	122.5	7.937	25.981

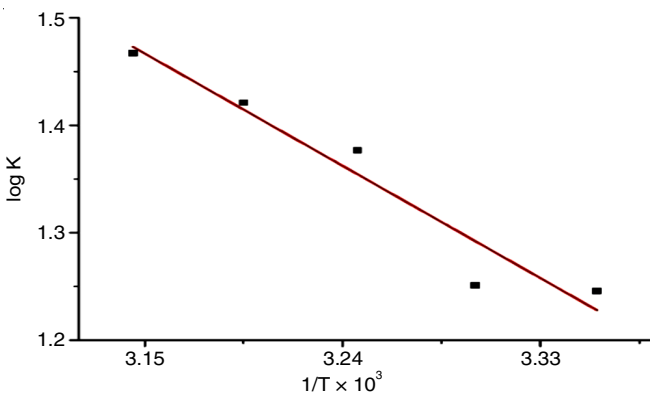

Fig. 7. Graph of log k *versus* $1/T \times 10^3$ for the complexation of Pr(III): L-valine in DMF at various temperatures

Conclusion

The reduction in the values of spin-orbit interaction (ξ_{4f}), Slater-Condon (F_k), Racah energy (E_k), and the increase in the values of nephelauxetic ratio (β), bonding parameter ($b^{1/2}$) and and percentage covalency (δ) reveals the complexation of praseodymium(III) with L-valine. When ligand was introduced to praseodymium(III), the band intensifies showing the interaction in the ligand orbital and the 4*f*-orbital of the metal which is also substantiated by the sharpening of the absorption bands and the appearance of the redshift. The decrease in the coordination number and the metal-ligand bond length of the complex formed were both related to the rise in absorption bands of the Pr(III):L-valine complex. The bonding parameter being positive

TABLE-7
COMPUTED OSCILLATOR STRENGTHS AND JUDD-OFELT INTENSITY PARAMETER FOR Pr(III): L-VALINE COMPLEX AT 313 K IN VARIOUS TIME (h) INTERVALS

Time (h)	$^3H_4 \rightarrow {}^3P_2$		$^3H_4 \rightarrow {}^3P_1$		$^3H_4 \rightarrow {}^3P_0$		$^3H_4 \rightarrow {}^1D_2$		t_2	t_4	t_6
	P_{obs}	P_{cal}	P_{obs}	P_{cal}	P_{obs}	P_{cal}	P_{obs}	P_{cal}			
0	6.545	6.545	1.856	1.663	1.456	1.657	2.765	2.765	203.34	4.545	20.167
2	6.667	6.667	1.967	1.847	1.612	1.723	2.824	2.824	211.23	5.123	20.567
4	6.834	6.834	2.135	1.945	1.678	1.865	3.167	3.167	234.12	5.245	20.978
6	7.143	7.143	2.255	1.989	1.734	1.967	3.264	3.264	253.53	5.476	21.698
8	7.367	7.367	2.354	2.076	1.785	2.007	3.312	3.312	263.56	5.672	22.543
10	7.545	7.545	2.513	2.231	1.813	2.089	3.398	3.398	266.78	5.895	23.276
12	7.788	7.788	3.624	2.651	1.667	2.654	2.491	2.491	47.45	7.653	23.645
14	7.945	7.945	2.383	2.176	1.925	2.234	3.541	3.372	243.65	5.954	24.521
16	8.097	8.097	3.765	2.454	1.168	2.482	2.685	2.685	66.164	6.734	24.634
18	8.234	8.234	3.945	2.564	2.018	2.234	3.576	3.576	271.56	6.324	25.321
20	8.347	8.347	4.056	2.676	2.148	2.567	3.661	3.661	93.76	7.543	25.865
22	8.564	8.564	4.067	2.686	2.216	2.573	3.765	3.765	276.38	6.989	26.182
24	8.672	8.672	4.112	2.645	2.292	2.587	3.812	3.812	316.31	8.143	26.586
26	8.784	8.784	4.256	2.731	2.307	2.671	3.883	3.883	-210.12	6.563	26.889
28	8.865	8.865	4.354	2.784	2.421	2.741	3.945	3.945	100.06	7.632	26.955
30	9.463	9.463	4.472	2.921	2.572	2.838	4.046	4.046	-298.34	4.731	29.987
32	9.651	9.651	4.512	3.029	2.463	2.678	4.134	4.134	-152.45	7.464	30.408
34	10.089	10.089	4.634	3.231	2.678	2.992	4.263	4.263	258.65	7.534	31.519

TABLE-8
COMPUTED OSCILLATOR STRENGTHS AND JUDD-OFELT INTENSITY PARAMETER FOR Pr(III): L-VALINE COMPLEX AT 318 K IN VARIOUS TIME (h) INTERVALS

Time (h)	$^3H_4 \rightarrow {}^3P_2$		$^3H_4 \rightarrow {}^3P_1$		$^3H_4 \rightarrow {}^3P_0$		$^3H_4 \rightarrow {}^1D_2$		t_2	T_4	t_6
	P_{obs}	P_{cal}	P_{obs}	P_{cal}	P_{obs}	P_{cal}	P_{obs}	P_{cal}			
0	6.134	6.134	1.745	1.543	1.321	1.456	2.524	2.524	202.56	4.321	20.123
2	6.345	6.345	1.881	1.673	1.387	1.515	2.637	2.637	209.23	5.112	20.654
4	6.543	6.543	1.964	1.733	1.398	1.567	2.721	2.721	231.12	5.267	20.862
6	6.767	6.767	2.015	1.890	1.406	1.589	2.798	2.798	243.52	5.321	21.701
8	6.911	6.911	2.165	1.947	1.435	1.625	2.835	2.835	254.61	5.546	22.683
10	7.058	7.058	2.223	2.001	1.487	1.664	2.905	2.905	258.07	5.786	23.465
12	7.286	7.286	2.299	2.104	1.502	1.697	3.023	3.023	46.56	7.543	23.870
14	7.457	7.457	2.383	2.156	1.563	1.722	3.112	3.112	241.52	5.872	24.324
16	7.631	7.631	2.523	2.266	1.599	1.776	3.234	3.234	64.124	6.931	24.701
18	7.886	7.886	2.741	2.198	1.627	1.855	3.345	3.345	270.61	6.573	25.253
20	8.049	8.049	2.956	2.564	1.709	1.902	3.427	3.427	91.62	7.497	25.907
22	8.278	8.278	2.989	2.645	1.785	1.996	3.491	3.491	271.33	6.831	26.342
24	8.542	8.542	3.009	2.667	1.831	2.045	3.532	3.532	314.55	8.432	26.671
26	8.781	8.781	3.078	2.692	1.891	2.098	3.589	3.589	-217.16	6.231	26.967
28	8.959	8.959	3.111	2.712	1.935	2.157	3.665	3.665	99.16	7.751	27.563
30	9.258	9.258	3.156	2.761	1.986	2.231	3.712	3.712	-297.84	4.645	29.675
32	9.573	9.573	3.179	2.795	2.021	2.354	3.755	3.755	-150.75	7.573	30.617
34	9.813	9.813	3.213	2.816	2.188	2.406	3.803	3.803	256.71	7.470	31.456

TABLE-9
RATE CONSTANT AND ACTIVATION ENERGY FOR THE COMPLEXATION OF Pr(III): L-VALINE AT VARIOUS TEMPERATURES

Temp. (K)	$1/T \times 10^3$	Rate constant	Rate constant (k)	Log k	ln k	Frequency factor (A)	Activation energy
298	3.3557	0.06341	17.614	1.24586	2.86869	17.98173	
303	3.3003	0.06418	17.828	1.25110	2.88077	18.19407	
308	3.2468	0.08573	23.814	1.37683	3.17027	24.29479	0.05119
313	3.1949	0.09494	26.372	1.42114	3.27230	26.89593	
318	3.1447	0.10556	29.322	1.46719	3.37834	29.89539	

and the growing value of Sinha's parameters (δ) implied the likelihood of covalent bonding in all situations where the nephelauxetic effect (β) value ranges from 0.944 to 0.947, which is less than unity. The correctness of the calculated data was predicted by the root mean square (RMS) values. The strong binding effect as well as the development of inner-sphere complexation in Pr(III):L-valine complex could be provided by the large fluctuations in the estimated readings of P and Ω_t.

TABLE-10
ACTIVATION ENERGY AND THERRMODYNAMIC FEATURES FOR Pr(III): L-VALINE COMPLEX AT VARIOUS TEMPERATURES

Temperature (K)	Rate constant (k)	ΔH	ΔG	ΔS	Activation energy 'E_a'
298	17.614		-7.13859	0.02402	
303	17.828		-7.34724	0.02413	
308	23.814	0.05119	-7.98780	0.02653	0.05119
313	26.372		-8.65303	0.02737	
318	29.322		-8.79295	0.02826	

With the oxygen and nitrogen donor ligands of L-valine, Pr^{3+} form a stable complex and through the inner sphere coordination, a nona-coordinated complex is formed. According to the assessed values of P and Ω_t parameters for the various organic solvents used, their sensitivity to the 4*f*-4*f* transition is in the following order: DMF > CH_3CN > $C_4H_8O_2$ > CH_3OH. According to the Arrhenius reaction, the rate of complexation calculated from the intensity parameters rises with increasing time and temperature. The low activation energy (E_a) indicated a fast reaction, the low readings of ΔG° illustrated the favourability and spontaneity of the reaction, whereas positive readings of ΔH° implied that the reaction is an endothermic reaction. The TΔS° > ΔH° revealed that the current research of complexation reaction is entropy-driven. Depending on how frequently molecules collide, the frequency factor (A) values show the important correlation between reaction rate and temperature.

ACKNOWLEDGEMENTS

The authors acknowledge the Department of Chemistry, Nagaland University, Lumami, India for providing the research laboratory facilities. One of the authors (Juliana Sanchu) is grateful to the UGC NON-NET fellowship, India for the financial support.

CONFLICT OF INTEREST

The authors declare that there is no conflict of interests regarding the publication of this article.

REFERENCES

1. A.M. Mãciucã, A.C. Munteanu and V. Uivarosi, *Molecules*, **25**, 1347 (2020); https://doi.org/10.3390/molecules25061347
2. J.A. Cotruvo Jr., *ACS Cent. Sci.*, **5**, 1496 (2019); https://doi.org/10.1021/acscentsci.9b00642
3. R.B. Martin and F.S. Richardson, *Q. Rev. Biophys.*, **12**, 181 (1979); https://doi.org/10.1017/S0033583500002754
4. K.B. Gudasi, V.C. Havanur, S.A. Patil and B.R. Patil, *Met. Based Drugs*, **2007**, 1 (2007); https://doi.org/10.1155/2007/37348
5. S. Alghool, M.S. Zoromba and H.F.A. El-Halim, *J. Rare Earths*, **31**, 715 (2013); https://doi.org/10.1016/S1002-0721(12)60347-0
6. M.P. Cabral Campello, E. Palma, I. Correia, P.M.R. Paulo, A. Matos, J. Rino, J. Coimbra, J.C. Pessoa, D. Gambino, A. Paulo and F. Marques, *Dalton Trans.*, **48**, 4611 (2019); https://doi.org/10.1039/C9DT00640K
7. J.V. Kuntal Prajapati, *Res. J. Life Sci. Bioinform. Pharm. Chem. Sci.*, **4**, 803 (2018); 10.26479/2018.0405.56
8. E.M. Stephens, S. Davis, M.F. Reid and F.S. Richardson, *Inorg. Chem.*, **23**, 4607 (1984); https://doi.org/10.1021/ic00194a040
9. S.N. Misra and M.I. Devi, *Biomol. Spectrosc.*, **53**, 1941 (1997); https://doi.org/10.1016/S1386-1425(97)00064-4
10. X.M. Qiao, C.X. Zhang, Y.K. Kong and Y.Y. Zhang, *Synth. React. Inorg. Met.-Org. Nano-Metal Chem.*, **46**, 841 (2016); https://doi.org/10.1080/15533174.2014.989594
11. S.N. Misra, G. Ramchandriah, M.A. Gagnani, R.S. Shukla and M.I. Devi, *Appl. Spectrosc. Rev.*, **38**, 433 (2006); https://doi.org/10.1081/ASR-120026330
12. N. Bendangsenla, T. Moaienla, T.D. Singh, C. Sumitra, N.R. Singh and M.I. Devi, *Spectrochim. Acta A Mol. Biomol. Spectrosc.*, **103**, 160 (2013); https://doi.org/10.1016/j.saa.2012.11.011
13. T.D. Singh, C. Sumitra, N. Yaiphaba, H.D. Devi, M.I. Devi and N.R. Singh, *Spectrochim. Acta A Mol. Biomol. Spectrosc.*, **61**, 1219 (2005); https://doi.org/10.1016/j.saa.2004.06.044
14. Y. Martínez, X. Li, G. Liu, P. Bin, W. Yan, D. Más, M. Valdivié, C.A.A. Hu, W. Ren and Y. Yin, *Amino Acids*, **49**, 2091 (2017); https://doi.org/10.1007/s00726-017-2494-2
15. K.K. Gangu, S. Maddila, S.N. Maddila and S.B. Jonnalagadda, *Molecules*, **21**, 1281 (2016); https://doi.org/10.3390/molecules21101281
16. F. Costanzo, R.G. Della Valle and V. Barone, *J. Phys. Chem. B*, **109**, 23016 (2005); https://doi.org/10.1021/jp055271g
17. A.L. Sobolewski, D. Shemesh and W. Domcke, *J. Phys. Chem. A*, **113**, 542 (2009); https://doi.org/10.1021/jp8091754
18. M.F. Bush, J. Oomens, R.J. Saykally and E.R. Williams, *J. Am. Chem. Soc.*, **130**, 6463 (2008); https://doi.org/10.1021/ja711343q
19. B.R. Judd, *Phys. Rev.*, **127**, 750 (1962); https://doi.org/10.1103/PhysRev.127.750
20. G.S. Ofelt, *J. Chem. Phys.*, **37**, 511 (1962); https://doi.org/10.1063/1.1701366
21. S.N. Misra and S.O. Sommerer, *Appl. Spectrosc. Rev.*, **26**, 151 (2006); https://doi.org/10.1080/05704929108050880
22. S.P. Sinha, Structure and Bonding in Highly Coordinated Lanthanide Complexes. In: Rare Earths. Structure and Bonding, Springer, Berlin, Heidelberg, vol 25, pp. 69-149 (1977); https://doi.org/10.1007/3-540-07508-9_3
23. W.T. Carnall, P.R. Fields and B.G. Wybourne, *J. Chem. Phys.*, **42**, 3797 (1965); https://doi.org/10.1063/1.1695840
24. P.D. Ross and S. Subramanian, *Biochemistry*, **20**, 3096 (1981); https://doi.org/10.1021/bi00514a017
25. M. Ziekhrü, Z. Thakro, C. Imsong, J. Sanchu and M. Indira Devi, *Polyhedron*, **200**, 115099 (2021); https://doi.org/10.1016/j.poly.2021.115099
26. J.B. Gruber, G.W. Burdick, S. Chandra and D.K. Sardar, *J. Appl. Phys.*, **108**, 023109 (2010); https://doi.org/10.1063/1.3465615
27. R.D. Peacock, The Intensities of Lanthanide *f-f* Transitions, In: Rare Earths. Structure and Bonding, Springer, Berlin, Heidelberg, vol 22 (1975); https://doi.org/10.1007/BFb0116556
28. N. Yaiphaba, *J. Chem. Pharm. Res.*, **5**, 377 (2013).
29. S.N. Misra and K. John, *Appl. Spectrosc. Rev.*, **28**, 285 (2006); https://doi.org/10.1080/05704929308018115
30. T. Moaienla, N. Bendangsenla and M.I. Devi, *Adv. Mater. Sci. Appl.*, **3**, 157 (2014); https://doi.org/10.5963/AMSA0303007
31. J. Burgess, Metal Ions in Solution, Ellis Horwood Distributed by Halsted Press, Chichester: New York (1978).